Silicon Reactivity at the Ag(111) Surface

Mauro Satta,[1] Stefano Colonna,[2] Roberto Flammini,[2] Antonio Cricenti,[2] and Fabio Ronci[2,*]
[1]CNR-Istituto per lo Studio dei Materiali Nanostrutturati, Dipartimento di Chimica, Università di Roma "La Sapienza", P.le Aldo Moro 5, I-00185, Roma, Italy
[2]CNR-Istituto di Struttura della Materia, Via Fosso del Cavaliere 100, I-00133 Roma, Italy
(Received 2 January 2015; revised manuscript received 4 April 2015; published 8 July 2015)

The modelization of silicene on Ag(111) is generally based on the assumption of a complete immiscibility between silicon and silver. However, there are recent reports that growth occurs inside the first layer of the Ag(111) terraces rather than on top of them. Here, we report on a combined density functional theory and scanning tunneling microscopy study unveiling the basic exchange mechanism between Si and the topmost layer Ag atoms and modeling the nucleation process. Our findings demonstrate that a strong Si-Ag interaction must be considered to properly describe the Si/Ag(111) interface.

DOI: 10.1103/PhysRevLett.115.026102 PACS numbers: 68.35.-p, 31.15.A-, 31.15.E-, 68.37.Ef

Silicene has been reported to be a novel silicon allotrope analog of graphene, theoretically predicted to be stable in the form of a freestanding two-dimensional layer with a buckled honeycomb structure [1–3]. Lately, based on the assumption that silicon and silver are immiscible at typical deposition temperatures, as suggested by the bulk binary Si-Ag alloy phase diagram [4], silicene synthesis has been reported to occur on Ag(111) [5,6], forming several different reconstructions [7–9]. The main point supporting silicene existence was the presence of linear electronic band dispersion in the vicinity of the Fermi level, attributed to Dirac cones. This point was recently questioned by several theoretical [10–14] and experimental [15–17] papers. Even the assumption of the Si-Ag immiscibility was very recently argued against by recent experimental studies on the Si/Ag(110) [18,19] and the Si/Ag(111) [20,21] interfaces. Indeed, in both cases Si atoms were observed to strongly interact with the Ag substrate, expelling Ag atoms and inducing reconstructions [18] or faceting [19], or growing reconstructed islands inside the first layer rather than on top of the substrate [20,21]. Surprisingly, silicon reactivity at the silver surface has never been considered in the theoretical calculations so far: all the studies reported in the literature are based on the initial assumption that the first silicon layer grows with a honeycomb structure on top of unreconstructed Ag(110) or Ag(111) substrates, with no other hypotheses being considered at all.

In this Letter we report on a combined theoretical and experimental study providing clear indications that Ag(111) is far from being an inert substrate for silicon. Indeed, in order to investigate the reactivity of evaporated atoms one has to take into account the energy released by the atom as adsorption takes place [22–24]. This excess energy can be dissipated by the system via two main different channels: through the phonon bath of the substrate or by inducing adatom mobility and/or reactivity at the surface [25]. By combining density functional theory (DFT) calculations and scanning tunneling microscopy (STM) measurements, we disclose the basic mechanism of silicon reactivity with the silver substrate. We demonstrate that a single silicon atom deposited on the Ag(111) surface does not merely adsorb on the surface but it may actually penetrate the first layer of the silver terrace, expelling a silver atom. The embedded Si atoms are confined in the first Ag(111) layer and act as seeds for the growth of the recessed reconstructed areas. The evidence reported in this Letter poses strong arguments against Ag(111) being an inert substrate for silicene growth and suggests that surface reactivity must be considered to understand and model the Si/Ag(111) system.

We started modeling the Si/Ag(111) interface by considering a single silicon atom interacting with a Ag(111) terrace. The two most stable adsorption sites for Si are the hcp ($T4$) and fcc ($H3$) hollow sites, as reported in Figs. 1(a) and 1(b), respectively. The resulting calculated Si adsorption energy value was $E_{\mathrm{ads}}^{\mathrm{Si}} \simeq 3.6$ eV for both sites, with a higher relative stability of 66 meV for the $H3$ site. Upon Si adsorption, the released energy $E_{\mathrm{ads}}^{\mathrm{Si}}$ can be dissipated by the system through different competing parallel processes: (i) it can be dispersed in the phonon bath of the silver bulk, (ii) it can promote the diffusion of the Si adatom on the Ag(111) surface, or (iii) it can be used by the Si atom to react with Ag atoms localized in the adsorption area. These different channels can be populated at different extents at the same time, the above processes having the same time scale [25]. A discussion of point (i) is beyond the aim of the present work, since a sophisticated dynamics multilevel methodology, such as the recent quantum mechanics on metals (QM/Me) approach [25], should be applied. We have thus focused our attention on points (ii) and (iii) by computing the energetics and by constructing reactive minimum energy paths (MEPs) of the more probable events. The results are reported in Fig. 1 and in Table I. In the Supplemental Material we provide details on the computational and experimental methods [26] and animations of the calculated structural changes occurring in the processes described below [30].

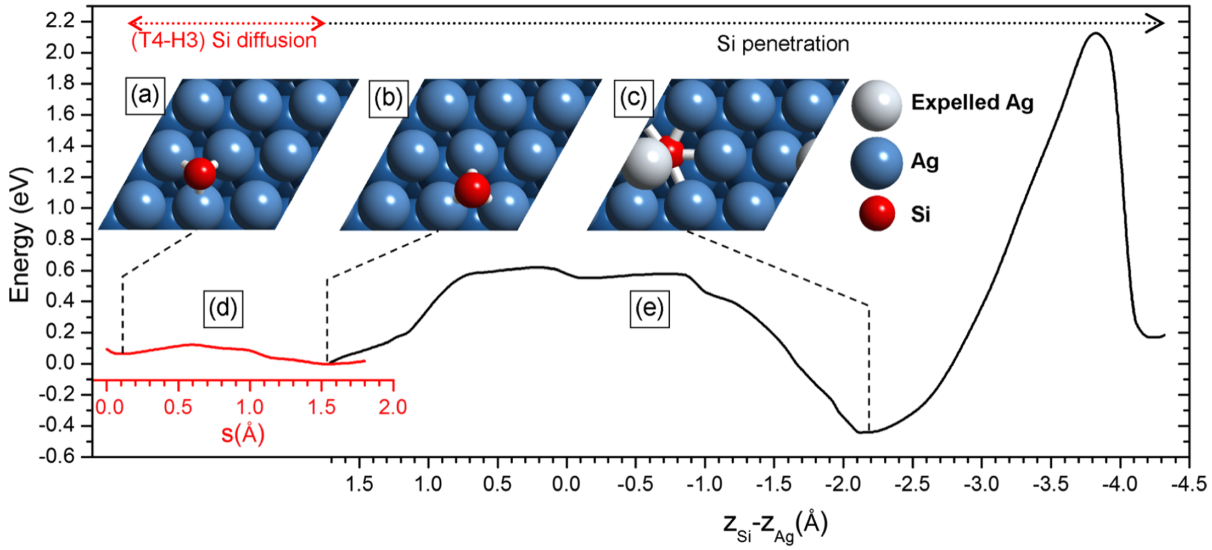

FIG. 1 (color online). Upper panels: relaxed structures of a Si adatom adsorbed at the (a) $T4$ or (b) $H3$ site. (c) Final relaxed structure of a Si atom substituting a 1st layer Ag atom. Lower panel: MEPs of the ($T4$-$H3$) Si diffusion process (d) and of the Si penetration process (e). See the Supplemental Material for details about the adopted reaction coordinates [26].

As a first step, we calculated the energetics of the diffusion process of a Si adatom moving from a $T4$ to a $H3$ adsorption site. The relative MEP connecting the two sites, reported in Fig. 1(d), is characterized by energy barriers of 0.058 and 0.124 eV for the forward and backward diffusion processes, respectively (see Table I). Since such energy barriers are much lower than $E_{\mathrm{ads}}^{\mathrm{Si}}$, Si adatom diffusion is expected to be easily attained, even considering that a significant amount of energy may be also dissipated via thermalization with the phonon bath of bulk silver.

We then considered the possibility that the excess energy $E_{\mathrm{ads}}^{\mathrm{Si}}$ may also be dissipated in reactive processes such as the penetration of the adsorbed Si atom into the Ag(111) surface. We studied the energetics of the Si penetration starting from the $H3$ site, given the higher stability with respect to the $T4$ site [Fig. 1(b)]. Given the higher stability of Si adsorbed at $H3$ sites, we studied the energetics of Si penetration starting from the model in Fig. 1(b). The relative MEP, reported in Fig. 1(e), shows a first energy barrier of 0.617 eV followed by an energy minimum at $(z_{\mathrm{Si}} - z_{\mathrm{Ag}}) \simeq 2.2$ Å, i.e., with the Si atom sitting ≃2.2 Å below the exchanged Ag atom, showing an energy decrease of 0.445 eV. Indeed, the relative structure, reported in Fig. 1(c), shows that silicon has penetrated the Ag(111) substrate, substituting for a Ag atom of the topmost layer. It is worth noting that the energy barrier of such an exchange process is far too high for a thermalized adatom to react: the exchange process occurs only thanks to the excess energy $E_{\mathrm{ads}}^{\mathrm{Si}}$ released by the adsorption process. A further penetration of the Si atom below the first Ag(111) layer is hindered by a much higher energy barrier of 2.567 eV, resulting in a less stable structure with an energy increase $\Delta E = 0.611$ eV, see Table I. Both the high energy barrier and the endothermic process make Si penetration below the first Ag(111) layer highly unlikely. On the other hand, the release of the embedded Si is also unfavored since the energy barrier for the reverse embedding reaction, Figs. 1(c) to 1(b), is sensibly high (see Table I) and the process would be endothermic as well. Once the Si atom has reached its embedded final state, the residual excess energy may in turn induce the diffusion of the expelled Ag atom. For this reason, starting from the structure in Fig. 1(c), we performed DFT calculations for computing the MEP of the Ag adatom separation process from the embedded Si atom. In the Supplemental Material we report the MEP [26] and the relative structure evolution animation [30], revealing that the process energetics consents the Ag adatom release from the embedded Si even at RT. A further system relaxation after removal of the adsorbed Ag adatom results in the stable structure reported in Fig. 2(h), in which the Si atom substitutes for a Ag atom of the topmost Ag(111) layer.

The above reported theoretical prediction about the Si-Ag exchange process has been experimentally verified by performing STM measurements at 80 K on very low coverage Si/Ag(111) samples obtained evaporating ≃1% of the Si amount required to achieve full coverage at RT. Figures 2(a) and 2(b) report empty state (ES) and filled state

TABLE I. Forward energy barrier ($\vec{E}_a$), reverse energy barrier ($\overleftarrow{E}_a$), and energy difference ΔE of the processes described in Figs. 1 and 3.

Process	$\vec{E}_a$	$\overleftarrow{E}_a$	ΔE (eV)
$T4$-$H3$ Si diffusion [Fig. 1(d)]	0.058	0.124	−0.066
Si penetration, 1st layer [Fig. 1(e)]	0.617	1.062	−0.445
Si penetration, 2nd layer [Fig. 1(e)]	2.567	1.956	+0.611
$T4$-$H3$ Si diffusion [Fig. 3(e)]	0.134	0.403	−0.269
Si penetration, 1st layer [Fig. 3(f)]	0.228	0.417	−0.189
$T4$-$H3$ Ag diffusion [Fig. 3(g)]	0.399	0.060	+0.339

(FS) images, respectively, showing the presence of several single defects as well as grouped defects. It is interesting to note that grouped defects made up of 2–5 atoms were never observed. The large majority of the single defects appear as dark (bright) round features in the ES (FS) images. In Figs. 2(c) and 2(d) we report ES and FS high resolution STM images of an 8×8 nm^2 area with two point defects, confirming the opposite appearance of such a kind of defect. By drastically reducing the gap voltage and increasing the tunneling current we were able to obtain an atomic resolution STM image of the very same 8×8 nm^2 area. This image, reported in Fig. 2(e), clearly shows that both defects are substitutional defects for Ag(111) terrace atoms, in full agreement with the calculated structure in Fig. 2(h). Furthermore, in Figs. 2(f) and 2(g) we report the simulated STM images of the structure in Fig. 2(h) at sample bias voltages +2 V (ES) and −2 V (FS), respectively. The good agreement between the experimental and simulated STM images confirms the hypothesis of the embedding process of the evaporated Si atoms substituting for Ag atoms at the Ag(111) first layer.

After considering the embedding process of a single Si atom, we extended our study, showing how additional Si atoms may be incorporated in the first Ag(111) layer to form clusters of embedded atoms. Assuming that the embedded Si atoms may act as seeds for the growth of the engraved islands, we considered the possibility that a thermalized Si adatom diffusing on the Ag(111) surface may exchange its position with a Ag atom in the proximity of an embedded Si atom [31]. The whole process, involving three consecutive steps, is illustrated in Fig. 3 and the relative structure evolution animations are reported in Supplemental Material [30]. Figure 3(e) shows the MEP of the diffusion process of the Si adatom approaching a $H3$ site near an embedded Si atom. The initial and final states are reported in Figs. 3(a) and 3(b), respectively. The MEP shows that this process is energetically favored, with a considerable total energy reduction $\Delta E = -0.269$ eV, see Table I. When the Si adatom reaches a $H3$ site adjacent to an embedded Si, Fig. 3(b), the most probable reactive process involves three atoms: the penetrating Si adatom pushes laterally the embedded Si atom, which, in turn, expels from the first layer a neighbor Ag atom. Interestingly, the MEP of this process, reported in Fig. 3(f), shows that the exchange energy barrier is reduced from 0.617 eV for the first embedding process to 0.228 eV for the second one (see Table I). In addition, the exchange process is demonstrated to be exothermic ($\Delta E = -0.189$ eV). The last reaction step is the distancing process of the expelled Ag atom, jumping from a $H3$ site adjacent to the embedded Si dimer to a $T4$ site of the Ag(111) surface, Figs. 3(c) and 3(d).

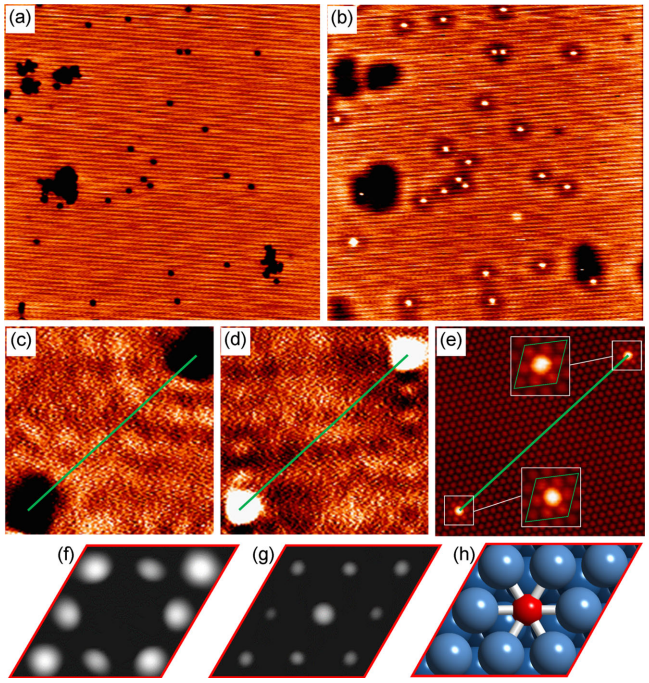

FIG. 2 (color online). Constant current STM images of an 1% full coverage Si/Ag(111) sample grown at RT. (a) ES and (b) FS 50×50 nm^2 STM images ($V_S = \pm 2$ V, $I_T = 2$ nA, $T = 80$ K). (c) ES and (d) FS 8×8 nm^2 STM images ($V_S = \pm 2$ V, $I_T = 10$ nA, $T = 80$ K). (e) High resolution STM image ($V_S = +3$ mV, $I_T = 25$ nA, $T = 80$ K) of the same area as (c) and (d). The green lines highlight the position of the two defects. Lower panels: simulated STM images at $V_S = +2$ V (f) and at $V_S = -2$ V (g) of the relaxed geometry of the embedded Si atom after removal of the exchanged Ag atom (h).

It must be noted that the Si adatom approach process in Fig. 3(e) is the bottleneck of the overall reaction, since its transition state is higher in energy than the following two. Since the energy barrier of the first MEP is of the same order of magnitude as the Si adatom diffusion energy barrier, the whole process is accessible even to Si adatoms thermalized at RT. Furthermore, considering the whole process from Figs. 3(a) to 3(d), a total energy difference of −0.119 eV is attained, indicating the higher stability of the final state.

As already noted above, STM measurements did not show the presence of such dimers, see Fig. 2(a). This evidence suggests that once an embedded dimer is formed, it will act as a seed for the rapid exchange reaction of the Si adatoms diffusing on the surface, resulting in the formation of progressively larger embedded structures. Eventually, all the impinging Si atoms will be embedded in the Ag(111) substrate, either directly upon adsorption or after diffusion and exchange at embedded clusters, giving rise to the reported formation of recessed islands and novel Ag(111) terraces [20,21].

The growth of islands embedded in the first substrate layer in etheroepitaxial systems has already been reported in the literature. In particular, this phenomenon was observed in binary systems showing very poor bulk miscibility, such as Au-Ni [32,33], Sb-Ag [34], Fe-Cu [35], Fe-Au [36], and Co-Cu [37] systems. In particular, the submonolayer deposition of Fe on Cu(100) shows results that are strikingly similar to the ones here reported for

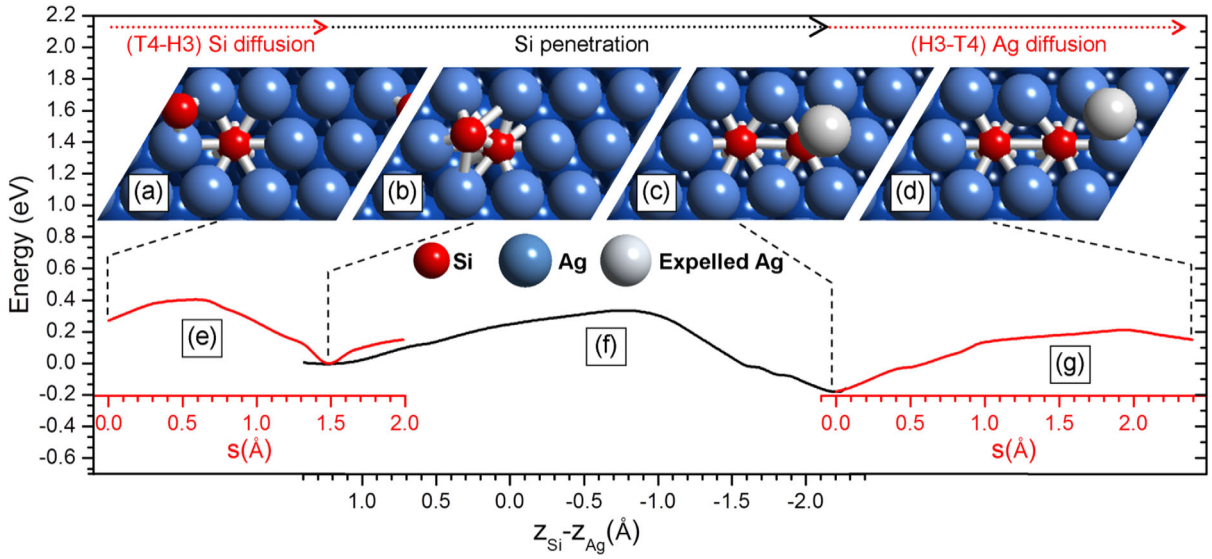

FIG. 3 (color online). Upper panels: relaxed structures of a Si adatom approaching an embedded Si atom from (a) a $T4$ site to (b) a $H3$ site, (c) relaxed structure after the Si-Ag exchange process, and (d) final structure after diffusion of the expelled Ag atom. Lower panel: MEPs of (e) the ($T4$-$H3$) Si diffusion process, (f) the Si-Ag exchange process, and (g) the Ag adatom diffusion. See Supplemental Material for details about the adopted reaction coordinates [26].

Si/Ag(111): both systems show bulk immiscibility, recessed island growth, and formation of novel substrate terraces resulting from the exchange mechanism between evaporant and substrate atoms. Fe inclusions in the first Cu(100) layer were reported to form through a single-atom nucleation process followed by growth induced by the progressive inclusion of Fe adatoms at the embedded nuclei [38]. In particular, it was demonstrated that the energy barrier for the exchange process of adatoms with the substrate atoms is strongly reduced as the size of the embedded clusters increases [39].

In the present study, we showed that both the total energies and the energy barrier decrease in passing from the embedding of the first Si to the embedding of the second Si (see Table I), making the exchange process possible even for thermalized adatoms. Consequently, in close analogy to Fe/Cu(100) [38,39], the energy of a system composed of one Si adatom plus an island of n Si embedded atoms is expected to be higher than the energy of a system composed of one Ag adatom and an island of $n+1$ Si embedded atoms (i.e., of the same system after Si-Ag exchange). Moreover, the probability that a wandering Si adatom will reach an embedded island increases with the island size and the energy barrier for the exchange process is expected to decrease as n increases, as in Fe/Cu(100) [38,39]. Hence, the Si-Ag exchange reaction occurs more rapidly as the size of the islands increases, causing the further embedding of the residual Si adatoms. As a result, the whole process gives rise to the reported formation of recessed islands and of novel Ag(111) terraces.

In summary, in this Letter we provide a description of the nucleation process at the Si/Ag(111) interface. By combining DFT and STM studies we demonstrate that, exploiting the excess energy released upon the adsorption process, the impinging Si atoms can penetrate the first silver layer and exchange position with Ag atoms. In the light of our study, the recently reported experimental observations of the Si/Ag(111) growth process now find a natural interpretation: the embedded Si atoms are confined in the first Ag(111) layer where they act as seeds for the growth of recessed islands. Our results demonstrate that surface reactivity cannot be neglected when describing the Si/Ag(111) interface formation.

The authors wish to thank the Narten Computational Facility in the Chemistry Department of Sapienza University. The technical support of G. Emma and M. Luce is warmly acknowledged.

*fabio.ronci@ism.cnr.it

[1] K. Takeda and K. Shiraishi, Theoretical possibility of stage corrugation in Si and Ge analogs of graphite, Phys. Rev. B **50**, 14916 (1994).

[2] G. G. Guzmán-Verri and L. C. Lew Yan Voon, Electronic structure of silicon-based nanostructures, Phys. Rev. B **76**, 075131 (2007).

[3] S. Cahangirov, M. Topsakal, E. Aktürk, H.Şahin, and S. Ciraci, Two- and One-Dimensional Honeycomb Structures of Silicon and Germanium, Phys. Rev. Lett. **102**, 236804 (2009).

[4] R. Olesinski, A. Gokhale, and G. Abbaschian, The Ag-Si (Silver-Silicon) system, Bull. Alloy Phase Diagrams **10**, 635 (1989).

[5] P. Vogt, P. De Padova, C. Quaresima, J. Avila, E. Frantzeskakis, M. C. Asensio, A. Resta, B. Ealet, and G. Le Lay, Silicene: Compelling Experimental Evidence for Graphenelike Two-Dimensional Silicon, Phys. Rev. Lett. **108**, 155501 (2012).

[6] L. Chen, C.-C. Liu, B. Feng, X. He, P. Cheng, Z. Ding, S. Meng, Y. Yao, and K. Wu, Evidence for Dirac Fermions in a Honeycomb Lattice Based on Silicon, Phys. Rev. Lett. **109**, 056804 (2012).
[7] B. Feng, Z. Ding, S. Meng, Y. Yao, X. He, P. Cheng, L. Chen, and K. Wu, Evidence of silicene in honeycomb structures of silicon on Ag(111), Nano Lett. **12**, 3507 (2012).
[8] R. Arafune, C.-L. Lin, K. Kawahara, N. Tsukahara, E. Minamitani, Y. Kim, N. Takagi, and M. Kawai, Structural transition of silicene on Ag(111), Surf. Sci. **608**, 297 (2013).
[9] P. Moras, T. O. Mentes, P. M. Sheverdyaeva, A. Locatelli, and C. Carbone, Coexistence of multiple silicene phases in silicon grown on Ag(111), J. Phys. Condens. Matter **26**, 185001 (2014).
[10] Z.-X. Guo, S. Furuya, J.-i. Iwata, and A. Oshiyama, Absence and presence of dirac electrons in silicene on substrates, Phys. Rev. B **87**, 235435 (2013).
[11] Y.-P. Wang and H.-P. Cheng, Absence of a dirac cone in silicene on Ag(111): First-principles density functional calculations with a modified effective band structure technique, Phys. Rev. B **87**, 245430 (2013).
[12] S. Cahangirov, M. Audiffred, P. Tang, A. Iacomino, W. Duan, G. Merino, and A. Rubio, Electronic structure of silicene on Ag(111): Strong hybridization effects, Phys. Rev. B **88**, 035432 (2013).
[13] P. Gori, O. Pulci, F. Ronci, S. Colonna, and F. Bechstedt, Origin of Dirac-cone-like features in silicon structures on Ag(111) and Ag(110), J. Appl. Phys. **114**, 113710 (2013).
[14] M. X. Chen and M. Weinert, Revealing the substrate origin of the linear dispersion of silicene/Ag(111), Nano Lett. **14**, 5189 (2014).
[15] C.-L. Lin, R. Arafune, K. Kawahara, M. Kanno, N. Tsukahara, E. Minamitani, Y. Kim, M. Kawai, and N. Takagi, Substrate-Induced Symmetry Breaking in Silicene, Phys. Rev. Lett. **110**, 076801 (2013).
[16] D. Tsoutsou, E. Xenogiannopoulou, E. Golias, P. Tsipas, and A. Dimoulas, Evidence for hybrid surface metallic band in (4×4) silicene on Ag(111), Appl. Phys. Lett. **103**, 231604 (2013).
[17] S. K. Mahatha, P. Moras, V. Bellini, P. M. Sheverdyaeva, C. Struzzi, L. Petaccia, and C. Carbone, Silicene on Ag(111): A honeycomb lattice without Dirac bands, Phys. Rev. B **89**, 201416 (2014).
[18] R. Bernard, T. Leoni, A. Wilson, T. Lelaidier, H. Sahaf, E. Moyen, L. Assaud, L. Santinacci, F. Leroy, F. Cheynis, A. Ranguis, H. Jamgotchian, C. Becker, Y. Borensztein, M. Hanbücken, G. Prévot, and L. Masson, Growth of Si ultrathin films on silver surfaces: Evidence of an Ag(110) reconstruction induced by Si, Phys. Rev. B **88**, 121411 (2013).
[19] F. Ronci, G. Serrano, P. Gori, A. Cricenti, and S. Colonna, Silicon-induced faceting at the Ag(110) surface, Phys. Rev. B **89**, 115437 (2014).
[20] J. Sone, T. Yamagami, Y. Aoki, K. Nakatsuji, and H. Hirayama, Epitaxial growth of silicene on ultra-thin Ag (111) films, New J. Phys. **16**, 095004 (2014).
[21] G. Prévot, R. Bernard, H. Cruguel, and Y. Borensztein, Monitoring Si growth on Ag(111) with scanning tunneling microscopy reveals that silicene structure involves silver atoms, Appl. Phys. Lett. **105**, 213106 (2014).
[22] J. Harris and B. Kasemo, On precursor mechanisms for surface reactions, Surf. Sci. **105**, L281 (1981).
[23] J. Barth, Transport of adsorbates at metal surfaces: from thermal migration to hot precursors, Surf. Sci. Rep. **40**, 75 (2000).
[24] H. Nienhaus, Electronic excitations by chemical reactions on metal surfaces, Surf. Sci. Rep. **45**, 1 (2002).
[25] J. Meyer and K. Reuter, Modeling heat dissipation at the nanoscale: An embedding approach for chemical reaction dynamics on metal surfaces, Angew. Chem., Int. Ed. **53**, 4721 (2014).
[26] See Supplemental Material at http://link.aps.org/supplemental/10.1103/PhysRevLett.115.026102 for computational and experimental details and the MEP of the Ag adatom separation process from the embedded Si, which includes Refs. [27–29].
[27] P. Giannozzi *et al.*, QUANTUM ESPRESSO: A modular and open-source software project for quantum simulations of materials, J. Phys. Condens. Matter **21**, 395502 (2009).
[28] J. Tersoff and D. R. Hamann, Theory of the scanning tunneling microscope, Phys. Rev. B **31**, 805 (1985).
[29] G. Boisvert and L. J. Lewis, Self-diffusion on low-index metallic surfaces: Ag and Au (100) and (111), Phys. Rev. B **54**, 2880 (1996).
[30] See Supplemental Material at http://link.aps.org/supplemental/10.1103/PhysRevLett.115.026102 for movies reporting the structural changes occurring upon the considered processes.
[31] The probability that a cluster of two embedded Si atoms may form, exploiting the adsorption energy $E_{\mathrm{ads}}^{\mathrm{Si}}$ of an incoming Si atom impinging on the surface in the proximity of an embedded Si atom, is obviously finite, but it is quite low and will therefore be ignored in this discussion.
[32] L. P. Nielsen, F. Besenbacher, I. Stensgaard, E. Laegsgaard, C. Engdahl, P. Stoltze, K. W. Jacobsen, and J. K. Nørskov, Initial Growth of Au on Ni(110): Surface Alloying of Immiscible Metals, Phys. Rev. Lett. **71**, 754 (1993).
[33] W. Cullen and P. First, Island shapes and intermixing for submonolayer nickel on Au(111), Surf. Sci. **420**, 53 (1999).
[34] S. Oppo, V. Fiorentini, and M. Scheffler, Theory of Adsorption and Surfactant Effect of Sb on Ag(111), Phys. Rev. Lett. **71**, 2437 (1993).
[35] K. Johnson, D. Chambliss, R. Wilson, and S. Chiang, A structural model and mechanism for Fe epitaxy on Cu(100), Surf. Sci. **313**, L811 (1994).
[36] O. Hernán, A. L. Vázquez de Parga, J. M. Gallego, and R. Miranda, Self-surfactant effect on Fe/Au(100):: place exchange plus Au self-diffusion, Surf. Sci. **415**, 106 (1998).
[37] R. Pentcheva, K. A. Fichthorn, M. Scheffler, T. Bernhard, R. Pfandzelter, and H. Winter, Non-Arrhenius Behavior of the Island Density in Metal Heteroepitaxy: Co on Cu(001), Phys. Rev. Lett. **90**, 076101 (2003).
[38] D. D. Chambliss and K. E. Johnson, Nucleation with a critical cluster size of zero: Submonolayer Fe inclusions in Cu(100), Phys. Rev. B **50**, 5012 (1994).
[39] R. C. Longo, V. S. Stepanyuk, W. Hergert, A. Vega, L. J. Gallego, and J. Kirschner, Interface intermixing in metal heteroepitaxy on the atomic scale, Phys. Rev. B **69**, 073406 (2004).